Resonant Instability of Laser Filaments in a Plasma

D. Pesme,[1] W. Rozmus,[2,3] V. T. Tikhonchuk,[4] A. Maximov,[2] I. Ourdev,[2] and C. H. Still[5]
[1]*Centre de Physique Théorique, Ecole Polytechnique, 91128 Palaiseau, Cedex France*
[2]*Theoretical Physics Institute, Department of Physics, University of Alberta, Edmonton T6G 2J1, Alberta, Canada*
[3]*Institute for Laser Science and Applications, University of California, Livermore, California 94550*
[4]*P. N. Lebedev Physics Institute, Russian Academy of Science, Moscow 117924, Russia*
[5]*Lawrence Livermore National Laboratory, Livermore, California 94550*
(Received 27 July 1999)

The stability of nonlinear laser light filaments in a homogeneous isothermal plasma with respect to coupled electromagnetic and density perturbations is examined. In addition to the previously known modulational instability of a trapped electromagnetic mode, a new fast growing resonant instability is found. It corresponds to the growth of an excited eigenmode in the waveguide formed by the filament density depletion, the associated density response being supersonic and transversally localized. The evolution of the instability is illustrated by numerical simulations in two and three spatial dimensions.

PACS numbers: 52.40.Nk, 52.75.Di, 52.35.Mw

The nonlinear evolution of randomized laser beams in laser produced plasmas is of ongoing concern in inertial confinement fusion studies and other applications of intense laser pulses, including x-ray sources and laser particle accelerators. Beam smoothing techniques have been designed to improve the uniformity of plasma illumination. They involve a random phase plate which breaks the laser beam into many independent beamlets whose interference pattern in the laser focal spot creates an ensemble of statistically independent speckles or hot spots. This improves the large-scale uniformity of the intensity pattern, but creates a speckle distribution with a significant number of large intensity hot spots, many times above the average value. These very intense small size hot spots give rise to nonlinear effects, which can alter the properties of a laser beam at a macroscopic level [1].

An individual hot spot evolves into a filament by forming an elongated density channel with trapped light propagating along its axis, provided that the laser light power within a speckle is above the critical value for self-focusing [2]. The equilibrium state of a nonlinear filament corresponds to a balance between the light ponderomotive and plasma pressures. Equilibrium filaments have been extensively discussed in the stationary approximation described by the nonlinear Schrödinger (NLS) equation [3].

It has long been known [4] that the validity of the stationary approximation is limited by a modulational instability, which involves the dynamical ion wave response. Modulational instabilities are nonresonant, involve long wavelength spatial perturbations, and develop on the corresponding long ion-acoustic time scale. Recent three dimensional simulations [5] have shown a new instability of a single nonlinear filament, which resulted in its total destruction on a much shorter time scale. This violent instability is analyzed in the present paper.

We explain the destruction of a filament by a new kind of resonant parametric instability, in which the fundamental mode of the waveguide formed by the filament density depletion is coupled to an excited eigenmode of this waveguide. This coupling involves a supersonic density response and displays similarities to strongly driven forward stimulated Brillouin scattering (SBS). However, contrary to forward SBS of plane waves or broad laser beams, the instability in a filament involves transversally localized modes and is characterized by a sharp maximum in the growth rate as a function of the wave number. This well-defined resonant wave number of the perturbation enables identification of the instability in simulations as well as allowing experimental verification.

Basic equations and stationary solutions.—The linearly polarized electromagnetic wave field, $\mathcal{E}$ is enveloped in space and time, $\mathcal{E}_y = \mathrm{Re}\{E \exp i(k_0 z - \omega_0 t)\}$, where ω_0 is the laser frequency, $k_0 = (\omega_0/c)\sqrt{1 - n_0/n_c}$ and n_0, n_c are the homogeneous background plasma density and critical density, respectively. Writing the total electron density n_e as $n_e = n_0(1 + n)$, the dynamical evolution of the perturbation n and of the electric field amplitude E is described in the paraxial approximation by the following system of equations:

$$(i\partial_z + iV_0^{-1}\partial_t + \nabla_\perp^2)E = nE\,, \qquad (\partial_{tt}^2 - \nabla_\perp^2)\ln(1 + n) = \nabla_\perp^2 |E|^2, \tag{1}$$

where $V_0 = \omega_{\mathrm{pe}}/2k_0 c_s$ is the dimensionless electromagnetic wave group velocity and ω_{pe} is the electron plasma frequency. The wave amplitude E is normalized to $\sqrt{16\pi n_c T_e}$, the coordinate z in the propagation direction is normalized to $2k_0 c^2/\omega_{\mathrm{pe}}^2$, the radial coordinate is normalized to the electron inertial length c/ω_{pe}, and time is measured in units of $c/c_s\omega_{\mathrm{pe}}$, where c_s is the ion acoustic velocity. The logarithmic term in the acoustic equation accounts for the saturation of the density response, and is necessary for the formation of equilibrium filaments.

Equilibrium solutions, $E = E_{\mathrm{eq}} \exp(i\lambda z)$, to Eqs. (1) can be found by solving an eigenvalue problem for the NLS equation, $\hat{L}E_{eq} = \lambda E_{eq}$, where $\hat{L} = \nabla_\perp^2 - n_{eq}(|E_{eq}|^2)$, and $n_{eq} = -1 + \exp(-|E_{eq}|^2)$ is the equilibrium density perturbation. Localized, axially symmetric solutions exist for $0 < \lambda < 1$. The limit $\lambda \to 0$ corresponds to the self-focusing threshold where the trapped power, $P = 2\int r dr |E_{eq}|^2$, equals the critical power, $P_c = 3.72$ [2,3]. The density perturbation n_{eq} represents a potential well for the electromagnetic wave, and $-\lambda$ defines the ground state energy level. A sufficiently deep potential well also admits excited states, which are solutions to the *linear* Schrödinger equation, $\hat{L}\delta E = \tilde{\lambda}\delta E$, for the electric field perturbation δE in the given density channel n_{eq}. These excited states, if present, can lead to a fast growing instability of the ground state.

Stability analysis of an equilibrium filament.—Consider solutions to the linearized Eqs. (1) describing the perturbations from the equilibrium state: $E = (E_{eq} + \delta E)\exp(i\lambda z)$ and $n = -1 + (1 + \delta N)\exp(-|E_{eq}|^2)$. Introducing an explicit dependence on the axial coordinate, azimuthal angle, and time, $(\delta N, \mathrm{Re}\delta E) = \mathrm{Re}[(N, E_R)\exp(im\phi + \Gamma t - iqz)]$, $\mathrm{Im}\delta E = \mathrm{Im}[E_I \exp(im\phi + \Gamma t - iqz)]$, one finds the following system of eigenmode equations:

$$(\hat{L}_m - \lambda)E_R - (q - i\Gamma/V_0)E_I = (1 + n_{eq})E_{eq}N\,,$$
$$(\hat{L}_m - \lambda)E_I - (q - i\Gamma/V_0)E_R = 0\,, \qquad (2)$$
$$(\Gamma^2 - \hat{L}_m - n_{eq})N = 2(\hat{L}_m + n_{eq})E_{eq}E_R\,,$$

where $\hat{L}_m = (1/r)\partial_r r \partial_r - m^2/r^2 - n_{eq}$.

The system (2) admits unstable solutions corresponding to the hoselike modulational instability in the long wavelength limit, $q \ll \lambda$. From the analysis of Ref. [5], one obtains the dispersion relation for the mode $m = 1$: $\Gamma^2 = A^2q^2$ where $A \approx 1/\sqrt{2\lambda}$ in the limit of a small amplitude filament, $\lambda \ll 1$. This leads to an estimate of the maximum growth rate, $\Gamma_{max} \sim \sqrt{\lambda}$, for $q \lesssim \lambda$.

A much faster growing supersonic instability can be found in the wavelength domain $q \lesssim \lambda$, in the presence of another trapped electromagnetic mode within the equilibrium density channel n_{eq}. It follows from the third equation of (2) that the density perturbation is small in the large growth limit, $|\Gamma| \gg 1$. Neglecting N in the first equation of (2) one obtains, in the first order approximation, a system of two equations for the electromagnetic wave amplitudes

$$(\hat{L}_m - \lambda)E_{R,I}^{(1)} - q_{res}E_{I,R}^{(1)} = 0\,. \qquad (3)$$

These are eigenvalue equations for the resonance wave number q_{res}, which corresponds to an excited eigenmode of the waveguide formed by the filament density depletion. Localized solutions require $0 < q_{res} < \lambda$, since λ corresponds to the ground state. The eigenvalue analysis of Eqs. (3) for $m = 1$ shows that there is no eigenstate other than the fundamental mode when $\lambda < 0.41$ (i.e., $P \lesssim 3P_c$), and there is an eigenstate $\lambda_1 = \lambda - q_{res}$ for filaments with larger intensity. By comparison, there is no threshold value for the antisymmetric mode in the two dimensional case often considered in simulations. The dependence of the eigenvalue λ_1 on P/P_c is shown in Fig. 1a. The eigenmode $E_R^{(1)}(r)$ for $\lambda = 0.5$ ($P/P_c = 4.24$) is shown in Fig. 1b. Higher excited levels appear in much more intense filaments. Levels with $m = 0$ (the mode with one node) and $m = 2$ exist for $\lambda \gtrsim 0.75$ ($P/P_c \gtrsim 18.7$), the next level $m = 1$ appears for $\lambda \gtrsim 0.8$ ($P/P_c \gtrsim 30.2$), and so on. We limit our discussion to the lowest excited level.

In the second order approximation the density perturbation follows from the third equation of (2):

$$N^{(2)} = (2/r\Gamma^2)(\partial_r r \partial_r - 1/r)E_{eq}E_R^{(1)}$$

and leads to a second order equation for the electric field assuming a small deviation $\Delta q = q - q_{res}$ from the resonance value. Since $\hat{L}_1$ is a self-adjoint operator, the dispersion equation is obtained by integrating a product of the second order equation and the first order eigenfunction with respect to a radial coordinate. This is $\Gamma^2(\Delta q + i\Gamma/V_0) = B$, where

$$B = \left(\int_0^\infty r\,dr[E_R^{(1)}]^2\right)^{-1}\int_0^\infty r\,dr(1 + n_{eq})\left[\frac{1}{2}\,\partial_r E_{eq}^2 \partial_r [E_R^{(1)}]^2 + (2\lambda - q_{res} + 2n_{eq})E_{eq}^2[E_R^{(1)}]^2\right].$$

The parameter B keeps relatively small values, $|B| \lesssim 0.1$, as a function of P/P_c, as shown in Fig. 1a. It changes sign from negative to positive for $P/P_c \approx 9$ ($\lambda \approx 0.64$). The maximum growth rate of the instability,

$$\Gamma_{max} = (1/2)(\sqrt{3} - iB/|B|)(|B|V_0)^{1/3}, \qquad (4)$$

corresponds to $\Delta q = 0$. The width of the resonance, $\Delta q_{res} \sim (|B|/V_0^2)^{1/3}$, is rather narrow for typical values of $V_0 \sim 10^3$.

The system (2) also has been solved numerically by using either a shooting method or by expanding the eigenfunctions in a series of $(m - 1/2)$ order Laguerre polynomials and computing the eigenvalues of the resulting matrix. Both methods produce the same results, the polynomial expansion being more robust and stable. Ten to twelve polynomials are sufficient to find the growth rate with an accuracy better than a few percent. A similar polynomial expansion has been used in the study of the hose instability of a short laser pulse within a plasma channel [6]. The results of Ref. [6] describing short pulse modulations involving fast electron response, Refs. [6,7], are similar to ours.

The dependence of the instability growth rate on wave number is shown in Fig. 1c for $P/P_c = 4.24$. The numerically calculated growth rate is in agreement with the analytical results presented above. There is no instability for short wavelengths corresponding to $q > q_{res}$.

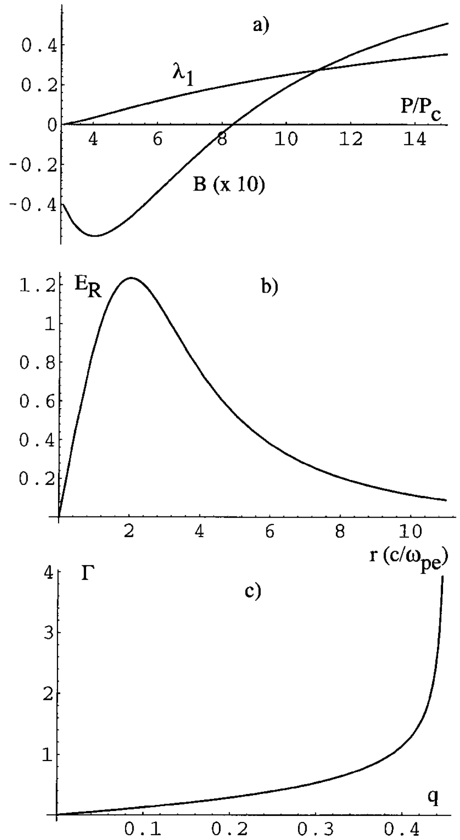

FIG. 1. (a) Dependence of the excited level λ_1 in the filament and the coupling coefficient B (magnified 10 times) for the resonance instability on the filament power, P/P_c. (b) Radial profile of the eigenfunction of the excited state $m = 1$ for $P = 4.24P_c$. (c) Dependence of the instability growth rate on the perturbation wave number for $m = 1$, $P = 4.24P_c$, and $q_{\rm res} = 0.46$.

In physical units the growth rate (4) can be written as $\Gamma \approx |B|^{1/3}\omega_0^{1/3}(\omega_{\rm pe}c_s/c)^{2/3}$, which is comparable to the growth rate for *backward* SBS in the strong coupling limit, and, therefore, is much larger than the maximum forward SBS growth rate for a homogeneous pump wave. In contrast with forward SBS, the large value of the growth rate found here is due to the lack of dependence on the small ratio $k_\perp/k_0 < 1$, where $k_\perp$ is the wave number of the ion acoustic wave participating in the forward SBS. In our case the short scale density perturbation is provided by the relatively small unstable filament radius, $a_0 \sim 2c/\omega_{\rm pe}$.

Numerical simulations of a single filament instability.—We have performed numerical simulations in two and three dimensional geometry using the nonparaxial wave interaction code [8] and the quasiparaxial code F3D [9]. In both codes the backward SBS is artificially suppressed by either strongly damping the SBS resonant ion-acoustic wave or by not solving the equation for the back-propagating wave. The results from the 2D nonparaxial code are presented in Fig. 2; the 3D results are similar and will be reported elsewhere.

Simulations start with a Gaussian laser beam being focused in the plasma and show the formation of nonlinear

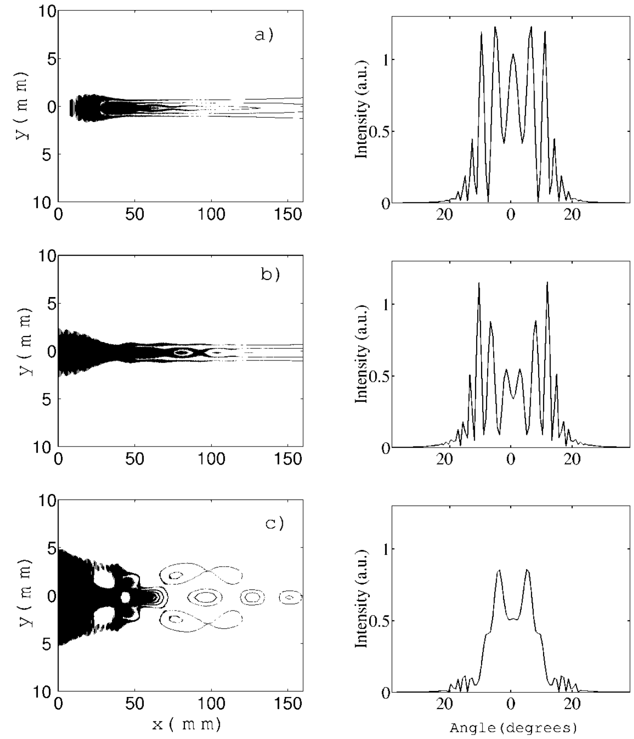

FIG. 2. Intensity contours and angular distributions of transmitted light at $t = 14.5$ ps (a), 18.2 ps (b), and 21.8 ps (c). At time $t = 0$ ps the 1 μm Gaussian beam has been focused in the center of the simulation box 100×160 μm^2 with maximum intensity 1.46×10^{15} W/cm^2 and FWHM 6 μm. The plasma parameters are $n_0/n_c = 0.4$ and $T_e = 1$ keV.

filaments which are similar to the equilibrium NLS solutions described before. Figure 2 demonstrates contours of light intensity in the interaction region at three different time moments illustrating filament formation, Figs. 2a and 2b, and the subsequent filament destruction, Fig. 2c. To the right of the intensity contour plots, far field images are shown for the same time moments. They display angular distributions of the transmitted light intensity. During the filament formation phase, angular distributions correspond to interference patterns of the coherent light emitted from the narrow structure which is created by the plasma density channel. The coherent pattern disappears, Fig. 2c, after rapid growth of the instability and filament disintegration. This is one of the signatures of plasma induced laser beam smoothing which is greatly enhanced by the instability of filaments.

The instability takes place at a time of 18–19 ps, and it is characterized by a fast growth rate, comparable with the theoretically found value of $\Gamma_{\rm max} = 1.2$ ps^{-1}. A modulation period of about 20–22 μm in Figs. 2b and 2c in the propagation direction is also in agreement with the results of linear theory, Eq. (4), giving $2\pi/q_{\rm res} \approx 20$ μm. Intensity maxima and their location away from the laser axis in Fig. 2c ($\sim$2 μm) correspond to the resonantly excited antisymmetric mode shown in Fig. 1b. Electric field phases differ by 180° at these maxima, i.e., at $x = 75$ μm and $x = 110$ μm.

Numerical simulations have shown that the instability is effectively destroying the filament. The interference between the fundamental mode and the excited modes produces a ponderomotive pressure which does not support the original density channel due to the complicated intensity pattern, Fig. 2c. Because of this instability, the light is detrapped and propagates in a wide interaction region.

Nonlinear filaments are formed over a relatively long time period, which equals the acoustic propagation time across the initial laser beam (18 ps in present simulations). It is therefore apparent that filament formation can occur without being interrupted by the resonant instability, in spite of the very short instability growth time. On the other hand, the solution to the eigenmode equation (2) indicates that the resonant instability cannot take place if the depth of the density channel is unsufficient to support an excited eigenmode. The necessary depth must be of the order of 90% of the density perturbation observed in the equilibrium filaments. This result explains both the relatively long time of filament formation and its fast disruption.

The dynamical evolution of a single filament produces a redshift in the transmitted light spectrum as shown in Fig. 3. An increasingly redshifted component corresponds to a time dependent phase shift, $\Phi = \int k_z dz$, of the electromagnetic wave propagating in a deepening density channel. This frequency shift, $\delta\omega = -\partial\Phi/\partial t \approx (k_0 L/2n_c)\partial n/\partial t$, characterizes the initial filament formation phase and continues until a time of 14 ps, when the channel formation slows down and the instability takes over. The maximum value of the redshift, ~1.5–2 nm, is many times above the magnitude which forward SBS could produce within the direction of propagation shown in Fig. 2. The density perturbations remaining after filament destruction propagate in the plasma, further enhancing the angular spread of the transmitted light (Fig. 2c) and forward SBS.

Conclusions.—The resonant instability of nonlinear filaments can play an important role in plasma induced beam smoothing effects and in turn in reducing the reflectivity of backward scattering instabilities. Long duration numerical simulations have shown quasiperiodic behavior after the initial explosion of the filament. The subsequent nonlinear evolution results in a smaller size of the secondary filaments, and the latter contain less power due to the dephasing effect produced by the remaining density fluctuations. The same fluctuations enhance forward SBS and the redshifted component of the transmitted light spectrum. Extrapolating the evolution of a single filament to the case of a multispeckle beam, one expects a reduction of the effective f-number and an increase in the temporal bandwidth of the transmitted light due to multiple laser filament disruptions. Such a behavior has been observed in recent large scale simulations in cases where the average speckle power is above the critical value for self-focusing. The instability of filaments could also be responsible for changes in the hot spot statistics by effectively destroying high power filaments.

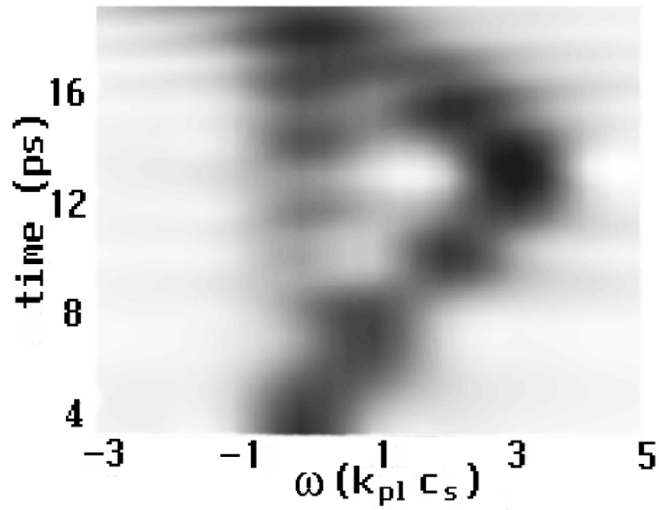

FIG. 3. Frequency spectrum of the transmitted light, which has been calculated within the window of 6 ps at different moments of time. Frequency is given in units of $k_0 c_s = 1$ ps^{-1} which corresponds to the wavelength shift of 0.57 nm.

The authors acknowledge helpful discussions and comments on the instability of guided laser beams by Robert Short. This work was partly supported by the Russian Foundation for Basic Research and by the Natural Sciences and Engineering Research Council of Canada. This work was partially supported under the auspices of the U.S. Department of Energy by the Lawrence Livermore National Laboratory under Contract No. W-7405-ENG-48. Part of this support was provided through the LLNL-LDRD program under the Institute for Laser Science and Applications. D. P. and W. R. would like to acknowledge support from the NATO Collaborative Research Grant, CRG 960770.

[1] H. A. Rose, Phys. Plasmas **2**, 2216 (1995).
[2] V. I. Talanov, Izv. Vyssh. Uchebn. Zaved. Radiofiz. **7**, 564 (1964); R. Y. Chiao, E. Garmire, and C. H. Townes, Phys. Rev. Lett. **13**, 479 (1964).
[3] L. Bergé, Phys. Rep. **303**, 259 (1998); F. Vidal and T. W. Johnston, Phys. Rev. Lett. **77**, 1282 (1996).
[4] V. E. Zakharov and A. M. Rubenchik, Sov. Phys. JETP **38**, 494 (1974); E. Valeo, Phys. Fluids **17**, 1391 (1974).
[5] V. V. Eliseev, D. Pesme, W. Rozmus, V. T. Tikhonchuk, and C. E. Capjack, Phys. Scr. **T75**, 112 (1998).
[6] G. Shvets and J. S. Wurtele, Phys. Rev. Lett. **73**, 3540 (1994); Ph. Sprangle, J. Krall, and E. Esarey, *ibid.* **73**, 3544 (1994).
[7] B. J. Duda and W. B. Mori (to be published).
[8] M. R. Amin *et al.*, Phys. Fluids B **5**, 3748 (1993).
[9] R. L. Berger *et al.*, Phys. Fluids **B5**, 2243 (1993).